Journal of Controlled Release 196 (2014) 79–86

Contents lists available at ScienceDirect

Journal of Controlled Release

journal homepage: www.elsevier.com/locate/jconrel

Targeted chelation therapy with EDTA-loaded albumin nanoparticles regresses arterial calcification without causing systemic side effects

Yang Lei, Nasim Nosoudi, Naren Vyavahare *

Department of Bioengineering, Clemson University, USA

ARTICLE INFO

Article history:
Received 8 August 2014
Accepted 29 September 2014
Available online 5 October 2014

Keywords:
Targeted EDTA chelation therapy
Elastin antibody
Medial calcification
Albumin nanoparticles
Arteriosclerosis

ABSTRACT

Background and aims: Elastin-specific medial arterial calcification (MAC) is an arterial disease commonly referred as Monckeberg's sclerosis. It causes significant arterial stiffness, and as yet, no clinical therapy exists to prevent or reverse it. We developed albumin nanoparticles (NPs) loaded with disodium ethylene diaminetetraacetic acid (EDTA) that were designed to target calcified elastic lamina when administrated by intravenous injection.

Methods and results: We optimized NP size, charge, and EDTA-loading efficiency (150–200 nm, zeta potential of −22.89 – −31.72 mV, loading efficiency for EDTA ~20%) for *in vivo* targeting in rats. These NPs released EDTA slowly for up to 5 days. In both *ex-vivo* study and *in vivo* study with injury-induced local abdominal aortic calcification, we showed that elastin antibody-coated and EDTA-loaded albumin NPs targeted the damaged elastic lamina while sparing healthy artery. Intravenous NP injections reversed elastin-specific MAC in rats after four injections over a 2-week period. EDTA-loaded albumin NPs did not cause the side effects observed in EDTA injection alone, such as decrease in serum calcium (Ca), increase in urine Ca, or toxicity to kidney. There was no bone loss in any treated groups.

Conclusion: We demonstrate that elastin antibody-coated and EDTA-loaded albumin NPs might be a promising nanoparticle therapy to reverse elastin-specific MAC and circumvent side effects associated with systemic EDTA chelation therapy.

1. Introduction

Vascular calcification occurs at two different sites—the intima and the media. Intimal calcification is generally associated with atherosclerotic plaques and inflammation; it can occlude the lumen. Medial arterial calcification (MAC), termed Monckeberg's sclerosis, is a type of vascular calcification disease that mostly occurs as linear deposits along elastic lamellae [1]. Vascular calcification, including MAC, is a strong predictor of cardiovascular morbidity and mortality [2]. Medial calcification, more prevalent in patients with chronic kidney disease (CKD) or diabetes, causes increased arterial stiffness. Surgical methods, such as directional atherectomy and stent grafts, are used to treat atherosclerosis and intimal calcification and to open occluded arteries [3,4]. However, there is no available treatment for elastin-specific MAC.

Chelation therapy, assumed to remove arterial calcification, is used primarily for intimal atherosclerotic calcification; however, very few animal studies have been performed, and none of the clinical studies has proven its effectiveness in improving cardiovascular function [5,6]. One clinical trial in the US from 2008 to 2013, Trial to Assess Chelation Therapy (TACT), aimed to determine the safety and effectiveness of EDTA chelation therapy by systemic infusion in individuals with coronary artery disease [7]. The results showed that an intravenous chelation regimen with EDTA modestly reduced the risk of adverse cardiovascular outcomes, but the study did not specifically show if EDTA chelation therapy could reverse vascular calcification [8]. Moreover, systemic chelation therapy using chelating agents such as EDTA or sodium thiosulfate to reverse calcification requires a high dosage and long treatment times, which cause side effects, such as hypocalcemia, bone loss, and renal toxicity [9–11]. For these reasons, chelation therapy is not approved by the US FDA.

Our previous studies showed EDTA might be a promising chelating agent to reverse elastin calcification both *in vitro and in vivo* when delivered close to the calcification [12]. However, systemic EDTA therapy delivered by intravenous injection did not show reversal of MAC [13]. Systemic delivery reduced blood calcium and increased urine calcium. These previous studies led us to develop a nanoparticle-based targeted chelating-agent delivery that could lower the dosage required and improve the bioavailability of the chelating agent [14]. We recently showed that elastin antibody-coated nanoparticles can be targeted to vascular calcification sites [15].

In this study, we tested if systemic delivery of targeted albumin NPs would deliver EDTA to the calcification site *in vivo*. We show reversal of

* Corresponding author at: Department of Bioengineering, Clemson University, 501 Rhodes Engineering Research Center, Clemson, SC 29634, USA. Tel.: +1 864 656 5558; fax: +1 864 656 4466.
E-mail address: narenv@clemson.edu (N. Vyavahare).

http://dx.doi.org/10.1016/j.jconrel.2014.09.029
0168-3659/

elastin-specific MAC with such NPs without the side effects associated with systemic EDTA chelation therapy.

2. Methods

2.1. Preparation of EDTA-loaded albumin NPs

Albumin NPs were prepared by the ethanol-desolvation method [16–18]. Briefly, 200 mg bovine serum albumin (BSA) was dissolved in 4 mL of distilled deionized water (DD water), and then the pH was adjusted to 8.5 with 6 N NaOH. EDTA was added to this solution at various concentrations (25, 50, 100, or 200 mg) for loading-optimization experiments. The aqueous solution was added drop-wise to 16 mL ethanol under probe sonication (20 Watts, Omni Ruptor 400 Ultrasonic Homogenizer, Omni International Inc, Kennesaw, GA) to prepare NPs. The particles were stabilized by fixation with 4% glutaraldehyde (100 μL) for 1 h and washed 3 times with DD water. The prepared NPs were then lyophilized and stored at 4 °C for further use. For NP tracking experiments, NPs were loaded with a fluorescent dye (2.5 mg, DiR, 1,1-dioctadecyl-3,3,3,3-tetramethylindotricarbocyanine iodide, Biotium, Inc., Hayward, CA) instead of EDTA (A flow chart for preparation of NPs is shown in online supplement Fig. 1 in the online-only Data Supplement).

2.2. Characterization of EDTA-loaded albumin NPs (details can be found in the online-only supplement)

Particle size and Zeta potential in suspension were determined using 90Plus Particle Size Analyzer (Brookhaven Instruments Co, Holtsville, NY). The EDTA loading efficiency was calculated using the formula:

$$\text{Loading efficiency}(\%) = \left(\frac{\textit{Amount of drug entrapped}}{\textit{Mass of nanoparticles recovered}}\right) \times 100 \quad (1)$$

In vitro EDTA-release studies were performed by incubating 2 mg EDTA-loaded albumin NPs in 1 ml of 0.1 M phosphate buffered saline (PBS) at pH 7.4 at 37 °C.

For cellular cytotoxicity concentrations of 100, 1000 μg EDTA-loaded albumin NP/ml cell-culture medium were used to evaluate possible toxicity to rat aortic smooth muscle cells (RASMCs, passage 6).

2.3. Demineralization of calcified tissue in vitro

Calcified porcine aortic elastin (160–180 μg Ca/mg tissue) was prepared by subdermal implantation of pure porcine-aortic elastin in rats as described in an earlier publication [19]. Calcified human aortas (100–300 μg Ca/mg tissue) from cadavers (age 49–75, both male and female with moderate or severe atherosclerosis) were received from the Greenville Health System (Greenville, SC) following an autopsy of cadavers. All samples were from the abdominal aorta, just below the renal arteries. As these samples came from autopsy and not linked to the patient information, IRB approval was not needed.

To determine the efficacy of EDTA-loaded albumin NPs to remove calcium from calcified tissue, calcified porcine-aortic elastin and separately calcified human aorta (10 mg each) were soaked in a 10 ml EDTA-loaded albumin NP dispersion (10 mg/ml in PBS, $n = 3$) with constant shaking at 37 °C. The control groups were soaked in 10 ml blank albumin NPs without EDTA loading (10 mg/ml in PBS, $n = 3$). At 3 days after treatment, all tissue samples were embedded in paraffin blocks, sectioned, and stained for qualitative analysis of calcium with Dahl's Alizarin red stain.

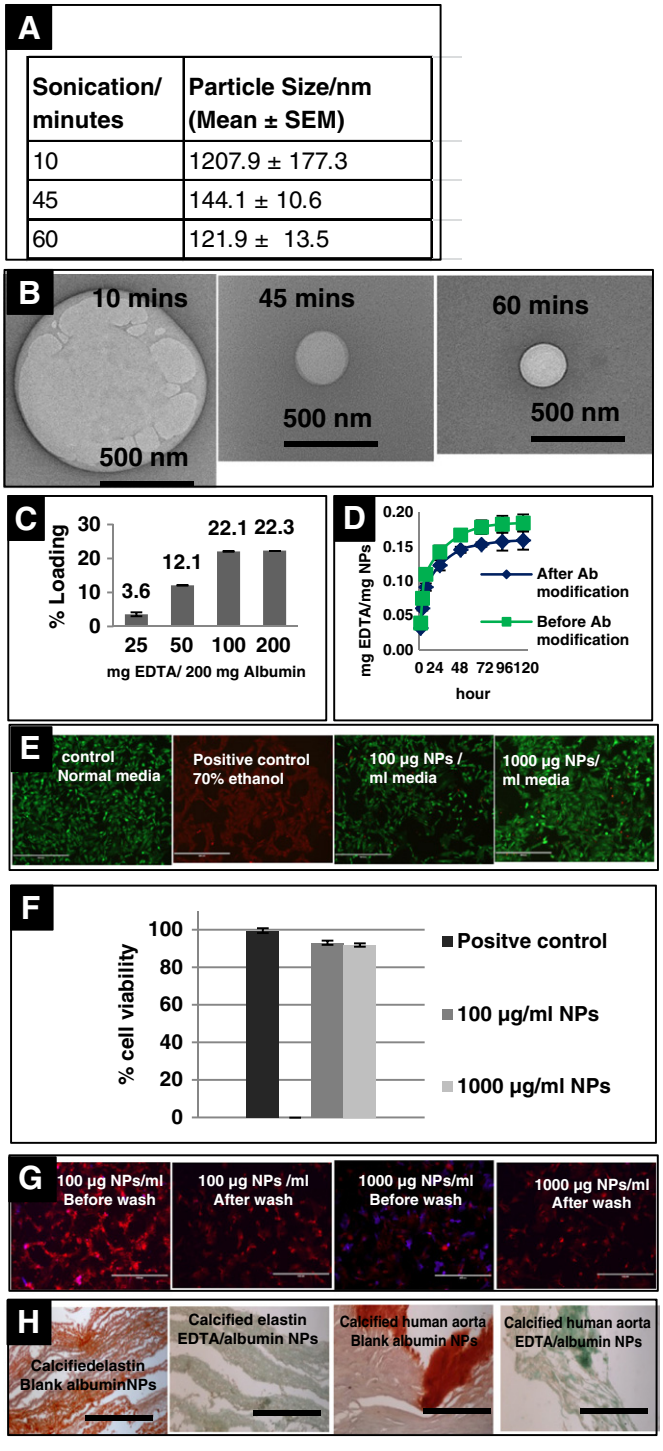

Fig. 1. Characterization for albumin NPs—optimization and function. A: Particle size measured by 90Plus Particle Size Analyzer with sonication times of 10, 45, and 60 min ($n = 3$). B: Images showing particle size measured by TEM with corresponding sonication times ($n = 3$).C: Loading efficiency with various EDTA to albumin ratios ($n = 3$). D: Release profile for EDTA-loaded albumin NPs before and after antibody modification ($n = 3$). Ab: antibody. E: LIVE/DEAD cell viability assay. Live control—normal medium; Dead control—treated by 70% ethanol; 100 μg NP/ml medium and 1000 μg NP/ml medium are two study groups ($n = 3$). Magnification: 100×. Scale bar: 400 μm. F: Cell viability determined by MTT assay ($n = 3$). G: Cellular uptake study with two NP concentrations of 100 μg NP/ml medium and 1000 μg NP/ml medium ($n = 3$). Red fluorescence: cell membrane stained by lipophilic membrane stain DiI (excitation/emission: 549/565 nm). Purple fluorescence: albumin NPs loaded with DiR near-infrared dye (excitation/emission: 745/810 nm). Magnification: 100×. Scale bar: 400 μm. H: Demineralization of calcified elastin and calcified human aorta with Blank albumin NPs without EDTA (control group) and EDTA-loaded albumin NPs ($n = 3$). Alizarin red stains calcium red (counterstained by light green stain). Magnification: 100×. Scale bar: 100 μm.

2.4. Antibody-coated, EDTA-loaded albumin NPs—preparation and optimization for antibody binding

Previous studies by others showed that NHS ester-PEG-maleimide had good efficiency to bind BSA and thiolated antibodies [18]. The antibody surface-coating strategy for albumin NPs is illustrated in online supplement Fig. 2. Antibody thiolation: 10 μg of antibodies was thiolated using 34 μg of freshly prepared Traut's reagent (G-Biosciences, Saint Louis, MO) in 0.1 ml PBS for 1 h. Antibodies used include Alexa-Fluor 555 goat anti-mouse IgG (Molecular Probes, Carlsbad, CA), rabbit anti-rat IgG antibody (Thermo Scientific, Rockford, IL) and rabbit anti-rat elastin antibody (United States Biological, Swampscott, MA). Thiolated antibodies were washed three times with PBS and dialyzed through 10 kDa MWCO filters to remove Traut's reagent.

Albumin NPs conjugated to maleimide-PEG-NHS ester: EDTA-loaded albumin NPs were prepared as described earlier. Albumin NPs were activated with heterobifunctional crosslinker α-maleimide-ω-N-hydroxysuccinimide ester poly (ethylene glycol) (Maleimide-PEG-NHS ester, MW 2000 Da, Nanocs Inc., NY, USA) to achieve a sulfhydryl-reactive particle system. Next, 2.5 mg of maleimide-PEG-NHS ester solution was added to 10 mg albumin NP dispersion. Then, the mixture was shaken for 1 h at room temperature.

Albumin NPs conjugated to antibodies: purified and thiolated antibodies were then added to the activated albumin NPs and incubated overnight at room temperature for conjugation. Samples were centrifuged, and the supernatant was analyzed using fluorescent spectrometry ($n = 3$). A calibration curve was plotted from standard solutions (0.1–25 μg of Alexa-Fluor 555 goat anti-mouse IgG in 1 ml of PBS). The bound dye was back-calculated by subtracting the amount of unbound dye in the supernatant. EDTA-loaded elastin antibody-coated NPs were labeled as EL-NP/EDTA and control EDTA loaded and IgG antibody coated NPs were labeled as IgG-NP/EDTA.

2.5. Immunostaining to visualize antibody binding to NPs

Rabbit anti-rat IgG antibody coated albumin NPs (IgG-NPs) were prepared as described earlier. A total of 0.1 ml of NPs (1 mg/ml) without antibody coating and IgG-NPs (2 μg IgG/mg NPs, 1 mg/ml) were incubated with 0.1 ml of 10 nm gold-stained goat-anti-rabbit IgG (Sigma Aldrich, St. Louis, MO) overnight in 0.01 M tris buffered saline (TBS), with 0.05% bovine serum albumin and 15% glycerol and 7.5 mM sodium azide. NPs were washed twice with TBS to remove unbound antibodies and NPs were obtained by centrifugation at 14,000 ×*g* for 15 min. Then 20 μl of NP suspension (1 mg/ml) was added on a formvar-coated copper grid and allowed to be dried overnight under reduced vacuum. Antibody surface conjugation was then analyzed by transmission electron microscopy (TEM).

2.6. In vivo nanoparticle targeting studies

A $CaCl_2$ injury model was used to induce local medial aortic calcification (MAC) at the abdominal aortic region following a previously reported protocol [12,20]. Briefly, 6 male Sprague–Dawley (SD) rats (6–8 weeks old) were anesthetized by 2–3% isoflurane. A ventral laparotomy exposed the peritoneal cavity. A 15 mm section of the infrarenal abdominal aorta was exposed, and injury was created by placing 0.5 M $CaCl_2$-soaked sterile cotton gauze on top of the aorta for 15 min. After $CaCl_2$ application, the gauze was removed, and the area was briefly flushed with warm saline. Incisions were then closed with continuous sutures (abdominal and subcutaneous) and surgical staples. Then, rats were allowed to recover and were maintained in standard chow conditions for one week. Animals were given buprenorphine (0.05 mg/kg) by subcutaneous injections daily for 3 days after surgery to minimize pain.

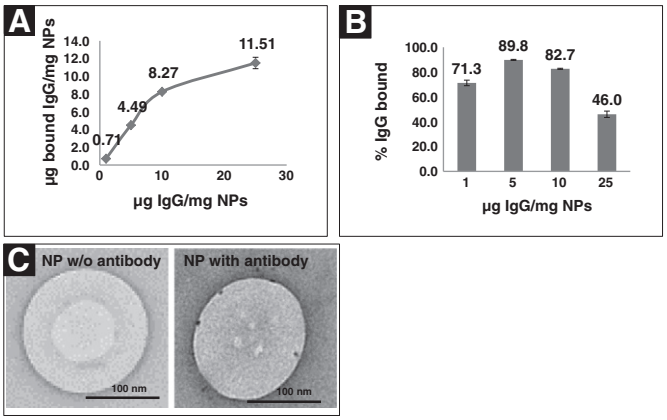

Fig. 2. Antibody binding and targeting efficacy *in vitro*. A: Amount of IgG antibody bound in 1 mg of albumin NPs with various starting ratios of antibody and albumin NPs ($n = 3$). B: Percentage of IgG antibody bound with albumin NPs with various starting ratios of antibody and albumin NPs ($n = 3$). C: Gold immune-stained albumin NPs TEM image ($n = 3$). Left: NPs without antibody coating as negative control. Right: NPs with IgG antibody coating, antibody concentration used: 2 μg/mg IgG-NPs. Small black dots on NP surface (right) represent 10 nm gold stained IgG.

After one week (when calcification in the injured site was observed), rats were anesthetized and DiR dye-loaded NPs (EL-NP/DiR or control IgG-NP/DiR) were injected through the tail vein (10 mg of NP/kg body weight in 0.1 ml saline). Rats were euthanized 24 h after the injection by CO_2 asphyxiation.

Only organs that showed a fluorescent signal were lyophilized and used to calculate biodistribution; these include aorta, heart, lung, liver, kidney, and spleen. No other organs or tissues, such as brain, muscle, skin, urine, and blood, had a detectable fluorescent signal.

Percentage of targeting for each organ was calculated as follows:

$$\%\text{targeting} = \left(\left(\frac{\text{fluorescence in aorta}}{\text{total fluorescence in all organs}}\right)\right)/(\text{dry weight of organ})) * 100$$

2.7. In vivo nanoparticle therapeutic-efficacy studies

An illustration of the experimental design for this animal study is shown in online supplement Fig. 3. The $CaCl_2$ injury described above was created (Day 0); this injury model develops local elastin-specific MAC. One week later, rats were divided into five groups for the following treatments by tail-vein injection (two times a week, two weeks): 1) saline as control group ($n = 5$); 2) high dose (HD) EDTA group ($n = 5$, 50 mg/kg EDTA); 3) low dose (LD) EDTA group ($n = 3$, 2.5 mg/kg EDTA); 4) IgG-NP/EDTA group ($n = 5$, 5 mg NP/rat/injection); 5) EL-NP/EDTA group ($n = 5$, 5 mg NP/rat/injection). Rats were placed in metabolic cages for urine collection for 24 h at the end of the treatment day (Day 21). Then, all rats were given another injection (depending on individual treatment groups) on Day 22, and urine samples were taken at time points of 1, 2, 3, and 4 h after injection and kept in −80 °C for further analysis. Immediately after urine collection, rats were euthanized by CO_2 asphyxiation, and organs were harvested, including the aorta (from the heart to the iliac bifurcation), blood, femoral bone, kidney, heart, liver, and spleen. Heparin (10 units/ml blood) was used as the anticoagulant for blood samples, and serum was removed and stored at −80 °C for further assay. The aorta, kidney, heart, liver, lung, and spleen were fixed in 10% buffered formalin for further analyses.

Aortic calcifications were evaluated by stereomicroscope (Leica M80 stereo microscope, Leica Microsystems Inc. Buffalo Grove, IL), microcomputed tomography (micro-CT) scanner (Siemens Inveon microPET/CT preclinical scanner, Siemens Healthcare Molecular

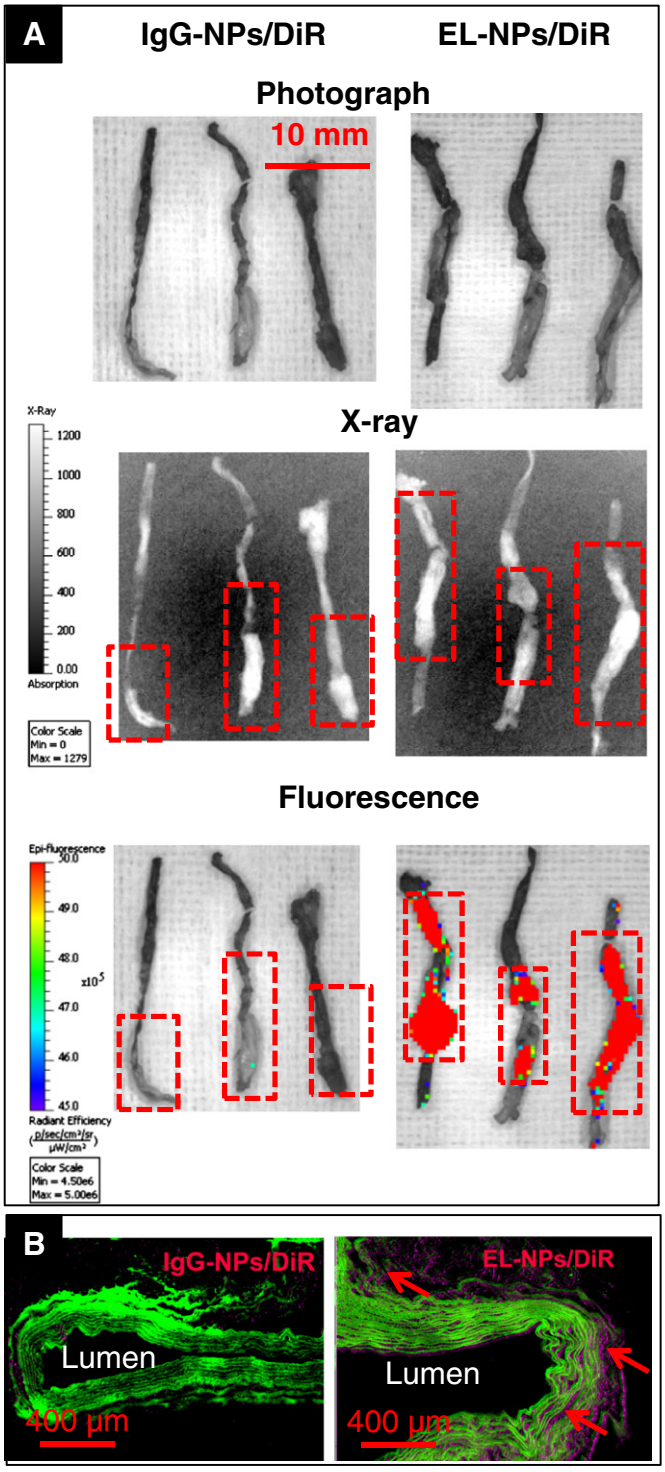

Fig. 3. Efficacy of DiR dye loaded NP targeting to damaged aorta *in vivo*. A: Photography, X-ray image and fluorescent image taken by IVIS image system ($n = 3$ in each treatment groups). IgG-NP/DiR: rabbit anti-rat IgG antibody modified albumin NPs loaded with DiR dye. EL-NP/DiR: rabbit anti-rat elastin antibody modified albumin NPs loaded with DiR dye. The red rectangle areas are calcified and damaged region detected by X-ray. High fluorescent signals were only found for EL-NPs group aortae suggesting targeting. B: Fluorescent microscopy of abdominal aorta from representative histological section ($n = 3$ in each treatment groups). Purple fluorescence: albumin NPs stained by DiR near-infrared dye (excitation/emission: 745/810 nm). Green fluorescence: auto-fluorescence from aortic tissue section. Left: aortic section from IgG-NP/DiR groups as control. Right: aortic section from EL-NP/DiR groups which indicated that EL-NPs had better targeting efficacy and could infiltrate from lumen to adventitia in damaged blood vessel. Red arrow indicated area where elastic lamina separated with more purple fluorescence.

Imaging, USA), histology, and atomic absorption spectrometry (AAS). Aortas from all rats were cleaned of all adherent tissues by blunt forceps after formalin fixation. Plastic tubing (PE, 1 mm outside diameter) was inserted into the cleaned aortas for easier handling during imaging. Whole aortas were imaged by a stereomicroscope (Leica M80 stereo microscope, Leica Microsystems Inc. Buffalo Grove, IL) both before and after Alizarin red staining [21–23]. Briefly, whole aortas were soaked in freshly made 2% Alizarin red solution (pH 4.1–4.3, pH) for 10 min and washed with distilled and deionized water for another 5 min. Then, aortas were imaged by stereomicroscope; and micro-CT for harvested aortas *in vitro* was based on a modified protocol [24,25]. Briefly, a 360-degree axial scan was collected at a peak tube potential of 80 kVp and a tube current of 500 uA. Data were reconstructed to 100 μm pixel size using a Feldkamp cone beam algorithm. Virtual 2D cross-sections and 3D maximum intensity projection views were created using MeVisLab software (MeVisLab, Mevis, Bremen, Germany, http://www.mevislab.de). Exported movies from MeVisLab were further edited by the video-editing software Corel VideoStudio Pro X7(Corel Inc, Mountain View, CA) (online-only video supplement 1).

Following the imaging by stereomicroscope and micro-CT scanner mentioned above, aortas were processed for histology with Alizarin red staining for visualization of calcium. The remaining parts of abdominal aortas were then used for Ca quantification by atomic absorption spectroscopy, AAS [12,26]. Briefly, ~2–10 mg of abdominal aortas were hydrolyzed in 1 ml of 6 N Ultrex HCl (Baker Company, Phillipsburg, NJ) and then resuspended in 0.01 N Ultrex HCl. Hydrolyzed samples were diluted and analyzed with AAS. Serum and urine samples were thawed and diluted before Ca quantification by AAS.

Femoral bones were dissected and fixed in 10% buffered formalin; their integrity was evaluated by micro-CT and by functional mechanical testing. Stiffness and maximum load were tested based on a three-point bending test. Micro-CT for femoral bones was done by the same protocol as the aortas, described above (one representative scan for all 2D-view slices from each group is available as online-only supplement Video 2). The three-point bending test was done using a Bose test instrument (Electroforce 3200, Bose, MN, USA) equipped with a 450 N load cell. First, stiffness was tested by measuring bone displacement in millimeters (mm) at a given force in newtons (N). Second, bones were exposed to higher force until fracture, and the maximum load N was determined.

All animal studies were approved by Clemson University Animal Ethics committee. The animal procedures conform to the NIH guidelines (Guide for the care and use of laboratory animals).

2.8. Statistical analysis

Results are expressed as mean ± standard deviation (SD). Statistical analyses of the data were performed using single-factor analysis of variance. Differences between means were determined using the least significant difference with an α value of 0.05. Asterisks in the figures indicate statistical significance ($P < 0.05$).

3. Results

3.1. Characterization for EDTA-loaded albumin NPs

NP size was dependent on sonication time; higher sonication time produced smaller NPs (Fig. 1A–B; $n = 3$). Our previous studies with polymeric NPs have shown that ~150–200 nm size particles enter through endothelium and bind to elastic lamina in the medial layers [15]. Thus all NPs intended for use in further studies were prepared by 45 min of probe sonication to obtain particles of ~150 nm size. EDTA-loading increased with the increase in EDTA concentration during NP preparation, but loading plateaued at ~22% (Fig. 1C; $n = 3$). The EDTA release profile for NPs showed an initial burst and then continuous

release for up to 5 days (Fig. 1D; $n = 3$) both before and after antibody modification. The amount of total EDTA was slightly lower after antibody modification because of loss of EDTA during antibody coating and washing steps. Zeta potential of NPs after antibody modification is shown in Table 1 ($n = 3$).

To target extracellular matrix elastin and reduce cellular uptake, all NPs were designed to be negatively charged (the mammalian cell membrane's inherent negative charge repels negatively charged particles) (Table 1). NPs were not taken up by RASMCs as shown by lack of purple staining within cellular cytoplasm after NP incubation and washing steps (Fig. 1G; $n = 3$). Cell toxicity was measured by placing EDTA-loaded albumin NPs in cell-culture medium. Live/Dead and MTT assays showed no RASMCs cell toxicity for 100–1000 μg NP/ml medium (Fig. 1E; F; $n = 3$).

Next we tested whether EDTA-loaded albumin NPs could remove calcium from calcified tissues *in vitro*. The NPs efficiently removed mineral both from calcified elastin and calcified human aorta samples (Fig. 1H; $n = 3$). The blank albumin NPs were unable to resorb calcification (Fig. 1H).

3.2. Antibody-coated EDTA-loaded albumin NPs—antibody binding and targeting efficacy in vitro

Antibody-binding yield was assessed by Alexa-Fluor 555-labeled IgG. The amount of antibody bound to albumin NPs increased with the increase in starting antibody concentration, and the bound percentage peaked around 5 μg IgG/mg albumin NPs (Fig. 2A–B; $n = 3$). Successful antibody coating was also verified by gold immune-staining under TEM, which showed 10 nm gold particles on the surface of the IgG-NPs (2 μg/mg IgG-NPs) and no gold particles on the control NPs without attached antibody (Fig. 2C; $n = 3$).

3.3. Efficacy of EL-NPs targeted to damaged aorta in vivo

DiR dye loaded NPs were delivered via tail vein injection and allowed to circulate for 24 h for biodistribution studies. Most of the DiR dye was permanently entrapped in albumin NPs, and thus fluorescence signal was used to quantify NP biodistribution. Gross photographs, X-ray images, and fluorescence for aortas are shown in Fig. 3A ($n = 3$ in each treatment groups). Areas where $CaCl_2$-mediated injury caused elastin damage and calcification showed significant fluorescence in the elastin antibody coated NP group (EL-NP/DiR) and no fluorescence for control IgG antibody coated NP group (IgG-NP/DiR). Representative histological sections for aortas from both EL-NP/DiR and IgG-NP/DiR treated groups showed that EL-NPs had better targeting efficacy and that NPs were distributed throughout media where elastin degradation and separation was observed suggesting the NPs could penetrate intact endothelium. Very little, if any, targeting was seen for control IgG antibody-coated NPs (Fig. 3B). When the fluorescent signal was quantified aorta, EL-NP-treated groups showed ~3 times more NP accumulation in calcification sites in the aorta (16.79% in EL-NPs versus 5.74% in IgG-NPs, $p < 0.05$, $n = 3$) and lesser amounts in spleen, kidney, lung, and heart when compared to control IgG-NP-treated groups (Table 2).

Table 1
Characterization of nanoparticles ($n = 3$).

Type of nanoparticle	Size ± SEM (nm)	Poly dispersity index	ζ-potential ± SD (mV)
IgG-NP/EDTA	177.9 ± 21.6	0.795	−22.89 ± 5.28
EL-NP/EDTA	144.1 ± 10.6	0.479	−31.72 ± 3.44

3.4. Therapeutic effects of targeted EDTA chelation therapy to reverse calcification

Aortic calcification for both systemic EDTA chelation therapy and targeted NPs based EDTA chelation therapy is shown in Fig. 4. Aortic calcification as evaluated stereomicroscopically before and after Alizarin red staining of the whole aorta showed significant reversal of aortic calcification in elastin antibody coated NPs (EL-NP/EDTA) group (Fig. 4A; $n = 5$). Four of five aortas showed complete reversal of calcification. While all five aortas showed significant persistence of calcification in control IgG antibody coated NPs (IgG-NP/EDTA) group (Fig. 4A). Histological staining of aortic cross-sections confirmed gross observations and showed significant reduction in elastic lamina calcification in the EL-NP/EDTA group and heavy calcification in the IgG-NP/EDTA group (Fig. 4B; $n = 5$). Calcium quantification in the aortas by AAS corroborated the staining results showing that EL-NP/EDTA group only had therapeutic effect of reversing aortic calcification and had the lowest level of Ca in the aorta (Fig. 4C, $P = 2.63E-06$, $n = 5$) From our previous reported data, calcium amount in healthy rats' aorta would be negligible [20]. When EDTA alone was delivered systemically by intravenous injection (without NPs), either in the same dose contained in NPs (2.5 mg/ kg, LD EDTA) or at twenty time that dose (50 mg/kg, HD EDTA), we found no reversal of calcification (Fig. 4C), which suggests that targeted therapy was essential for reversing calcification. Micro-CT data for whole aorta showed calcified regions in all groups except EL-NP/EDTA group (online-only video supplement 1.

3.5. Targeted EDTA chelation therapy did not have side effects associated with systemic EDTA chelation therapy

Possible side effects with both systemic EDTA chelation therapy and targeted EDTA chelation therapy are shown in Figs. 5 ($n = 5$) and 6 ($n = 5$). Results showed no side effects in EL-NP/EDTA-targeted chelation therapy group for serum and urine Ca as seen in high dose systemic EDTA treated group (Fig. 5A–C). In all groups, no changes were seen in bone morphology or stiffness and fracture stability (Fig. 6A–C). Notably, EDTA-treated groups had slightly higher maximum load than the untreated group (Fig. 6C, $P = 0.0273$, $n = 5$). Micro-CT data for femoral bones did not show any bone defects or loss in all groups (online-only supplement Video 2). EDTA treatments did not induce renal toxicity in any groups (online supplement Fig. 4) such as renal tubular vacuolization and pinocytosis as shown by others for long-term EDTA therapy [10,27–31].

4. Discussion

To our knowledge, this is the first time it has been shown that targeted nanoparticles injected systemically can bind to calcified arteries and regress calcification *in vivo*.

Our goal was to test if elastin-specific MAC can be removed by targeted chelation therapy. We chose EDTA because our previous comparative study of three chelating agents (EDTA, sodium thiosulfate and DTPA (diethylene triamine pentaacetic acid)) showed that

Table 2
Organ distribution of fluorescent nanoparticles ($n = 3$ in each treatment groups).

Organ	% total fluorescence/g dry weight (IgG-NP/DiR)	% total fluorescence/g dry weight (EL-NP/DiR)
Aorta	5.74 ± 0.45	16.79 ± 3.05
Liver	32.65 ± 1.95	36.31 ± 5.47
Spleen	35.46 ± 2.63	31.06 ± 3.92
Kidney	14.41 ± 1.79	11.50 ± 1.99
Lung	6.81 ± 0.50	3.38 ± 0.18
Heart	4.94 ± 3.16	1.72 ± 0.46

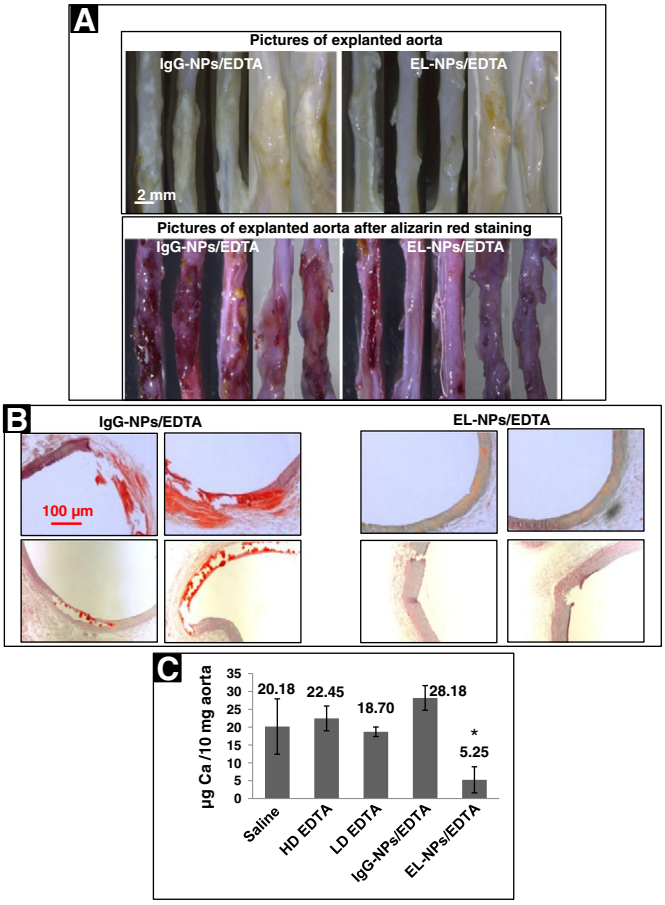

Fig. 4. Evaluation of aortic calcification for both systemic EDTA chelation therapy and targeted EDTA chelation therapy. A: Aortic calcification evaluated by stereomicroscope before and after whole aorta's Alizarin red stain for control IgG antibody coated and EDTA loaded NPs (IgG-NP/EDTA) and elastin antibody coated and EDTA loaded NPs (EL-NP/EDTA) groups ($n = 5$). B: Histological stain by Alizarin red for IgG-NP/EDTA and EL-NP/EDTA groups ($n = 5$). C: Ca quantification in aorta by AAS for all five treatment groups ($n = 5$/group). HD EDTA: 50 mg EDTA/kg dose, LD EDTA: 2.5 mg EDTA/kg dose.* Only EL-NP/EDTA was statistically lower in value than any other group.

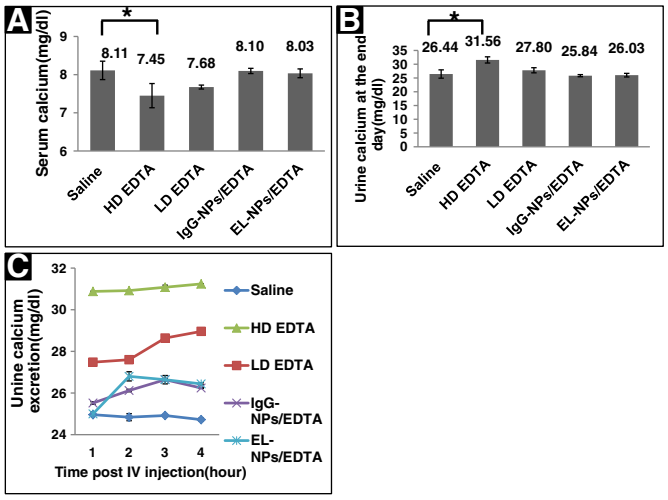

Fig. 5. Analyses of serum and urine calcium. A: Serum Ca quantification for all five treatment groups (HD EDTA group showed significant reduction in Ca, $P = 0.0045$, $n = 5$). Blood samples were collected on Day 22 after CO_2 asphyxiation. B: Urine Ca quantification for all five treatment groups (HD EDTA group showed significant increase I Ca, $P = 0.0001$, $n = 5$). Urine samples were also collected on Day 22 (24 hours' urine volume) before the final injection. C: Kinetics of Ca in urine after tail vein injection of EDTA and nanoparticles ($n = 5$).

EDTA was the most effective at removing calcium from hydroxyapatite and calcified tissue [12]. In the same study, we showed that local placement of EDTA-loaded poly(lactic-co-glycolic) acid (PLGA) nanoparticles on top of a calcified aorta could effectively reverse elastin-specific MAC in a rat calcification model [12]. However, such an invasive procedure cannot be translated for human use. In an attempt to target drugs to diseased arteries, we recently found that specifically designed NPs with elastin-targeting antibodies on the surface were able to deliver agents to the site of elastic-lamina damage [15]. In healthy arteries, the surface of elastin fibers in elastic lamina is covered with microfibrillar glycoproteins such as fibrillins, fibulins, and matrix Gla protein (MGP); thus, the elastic lamina is not accessible to elastin-targeted antibodies in healthy arteries. In most vascular diseases, the elastic lamina becomes damaged and the amorphous core elastin is exposed due to enzymatic degradation of microfibrillar proteins. That provided us the opportunity to create NPs specifically targeted to arterial-disease sites by coating them with antibody for core elastin [15]. These previous studies led to our designing an elastin-antibody coated EDTA-loaded albumin NP to reverse elastin-specific MAC and avoid side effects associated with systemic EDTA chelation therapy. We chose albumin nanoparticles instead of polymeric nanoparticles (e.g., PLGA) because albumin NPs are less toxic as no organic solvents are used in their preparation and they are frequently used in clinical applications [17,32]. Furthermore, we were also able to load significantly higher amounts of EDTA in albumin NPs rather than in PLGA NPs due to EDTA–albumin interactions.

We optimized the surface charge and size of albumin NPs so that they could penetrate the endothelium and bind to the degraded elastic lamina. The size of EDTA-loaded albumin NPs was dependent on the duration of sonication time, and we found that 45 min of probe sonication resulted in 150–200 nm size required for penetration through endothelium. Others have shown that particle sizes less than 100 nm had greater uptake by vascular smooth muscle cells [33]. Particles larger than 500 nm cannot effectively penetrate vascular endothelium or basement-membrane vessels [33]. Our previous results indicated that nanoparticles of ~200 nm were able to penetrate both the endothelium and the basement membrane [15]. The particle charge was kept negative to minimize cellular uptake. Since the mammalian-cell membrane has a negative charge, negatively charged particles are less likely to be taken up by cells [34]. Our results showed that 150–200 nm albumin NPs with a negatively charged surface penetrated the endothelium and were bound to the damaged elastic lamina with limited uptake by cells. EDTA-loaded NPs released EDTA for up to 5 days. We found that EDTA-loaded albumin NPs did not cause significant cell death or cellular uptake. To determine whether such NPs could remove calcium from calcified elastin and human aortas *in vitro*, we incubated EDTA-releasing NPs with calcified tissues; they removed calcium from both calcified elastin and calcified human aorta *in vitro*. Having tested the charge and size and targeting and therapeutic efficacy *in vitro*, we designed *in vivo* experiments to test if such NPs could deliver EDTA to calcified aorta under the high shear blood-flow conditions of the aorta. We injected NPs through the rat tail vein and allowed them to circulate and target to the sites. NPs (loaded with DiR dye) with elastin antibodies on the surface (EL-NP/DiR) did accumulate at the injured aortic site; control IgG antibody-coated NPs (IgG-NP/DiR) did not. More importantly, NPs accumulated only at damaged elastic lamina at the calcified site and did not target healthy vasculature. Our reported ~16% of the targeted dose was calculated first by normalization to organs' weights. As the weight of the calcified aorta is significantly

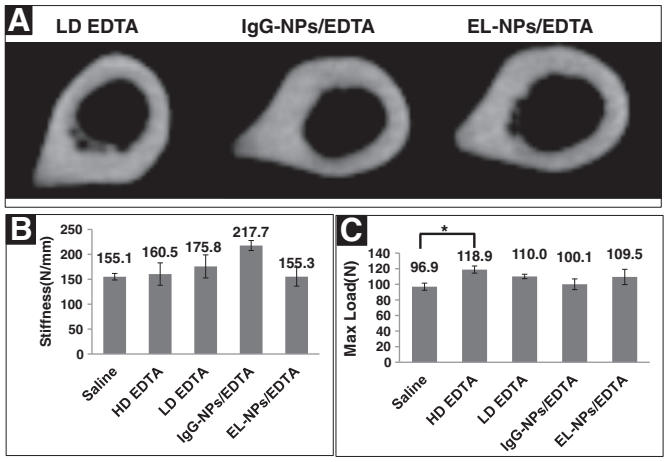

Fig. 6. Analyses of bone integrity ($n = 5$). A: Bone morphology analyzed by Micro CT showing 15 mm below the trochanter major of femoral bone. B: Stiffness of femoral bone for all five treatment groups. C: Maximum load of femoral bone for all five treatment groups (HD EDTA group showed significant increase, $P = 0.027$, $n = 5$).

lower than other organs, it shows higher percentage. Nahrendorf et al. have also normalized targeting to tissue weight and only showed 5% targeting to the aorta for imaging macrophages in inflammatory atherosclerosis [35]. If we look at the total targeting of all NPs delivered systemically, our targeting was ~2% for EL-NP/DiR group while only 0.5% for IgG-NP/DiR group.

Having confirmed targeting efficacy of NPs, we then injected NPs containing the chelating agent EDTA with either elastin antibody on the surface (EL-NP/EDTA) or as a control irrelevant IgG antibody coated NPs (IgG-NP/EDTA) in a separate set of rats. We chose to inject NPs twice weekly based on the *in vitro* release profile for EDTA. Within 2 weeks of injections (4 injections in total), we observed complete removal of calcium from 4 of 5 arteries in the EL-NPs EDTA group as confirmed by Alizarin red staining, micro-CT, and quantitative calcium scores. Not only was calcium removed, but the elastic lamina appeared to be less damaged (shown in histological section) after removal of calcium. As expected, EDTA-loaded control IgG antibody coated NPs did not target the sites and did not remove calcium. When EDTA alone was injected systemically either in high dose (similar to what is used clinical studies) or low dose (based on how much total EDTA was delivered through NPs), calcification was not resorbed as assessed by Alizarin red staining, quantitative calcium results, and micro-CT experiments. Moreover, we found that an EDTA dose similar to that used clinically (50 mg/kg) caused significant adverse events for serum and urine calcium: hypocalcemia and hypercalciuria, respectively [13]. Our NPs contained 20 times lower EDTA (which was protected in albumin NPs), and it was released slowly over a period of five days. Thus, we did not find any systemic toxicity for nanoparticle groups. These results indicate that elastin-antibody-coated and EDTA-loaded albumin NPs might be a promising nanoparticle therapy to reverse elastin-specific medial calcification. Because this targeted nanoparticle-delivery method would lower the dosage required for the chelating agent EDTA, side effects associated with systemic intravenous infusion, such as hypocalcemia and bone loss, could be avoided [9–11]. Antibody-mediated tissue targeting of albumin NPs for clinical practice has been approved by the FDA for other drugs [36,37], so our antibody coated albumin NPs have great potential clinical relevance.

5. Limitations of our study

Our study has some limitations. First, our EDTA chelation therapy was performed for a period of only two weeks. We do not know if calcification will return after halting the therapy. Second, we did not investigate possible side effects besides serum calcium, urine calcium, and bone loss. More kidney functional evaluation might be necessary such as serum creatinine level. Finally, we evaluated EDTA chelation therapy in a rat $CaCl_2$ injury model, which induced MAC at the site of injury. Patients have calcification dispersed throughout the arterial tree; thus animal models such as warfarin [21] or vitamin D [38] application where calcification is seen at various places such as aortic arch and renal and femoral bifurcation should be used in future in order to investigate EDTA chelation therapy's therapeutic effects. Careful risk–benefit analysis needs to done before use in individual human patients.

6. Conclusions

We prepared EDTA-loaded albumin NPs with an optimized size of 150–200 nm, zeta potential of −22.89 – −31.72 mV, EDTA loading-efficiency of ~20%, and sustained release for up to 5 days. Both *ex vivo* study and *in vivo* study using an aortic calcification model showed that elastin-antibody-coated, EDTA-loaded albumin NPs have good targeting efficacy and can reverse elastin-specific medial calcification. EDTA-loaded albumin NPs did not cause the side effects of calcium in serum and urine that are seen in high-dose EDTA-treated groups. No treatment groups showed bone loss. Elastin-antibody-coated, EDTA-loaded albumin NPs might be a promising nanoparticle protein engineered therapy to reverse calcification in elastin-specific medial calcification and circumvent side effects associated with traditional systemic EDTA chelation therapy by intravenous infusion.

List of non-standard abbreviations and acronyms

AAS	atomic absorption spectroscopy
Ab	antibody
AF	Alexa-fluor
DiR	1,1-dioctadecyl-3,3,3,3-tetramethylindotricarbocyanine iodide
DMSO	dimethyl sulfoxide
DD water	distilled and deionized water
ECM	extracellular matrix
EDTA	disodium ethylene diaminetetraacetic acid
EL-NPs	rabbit anti-rat elastin antibody coated albumin NPs
IgG	immunoglobulin G
IgG-NPs	rabbit anti-rat IgG antibody coated albumin NPs
MAC	medial arterial calcification
MAGPs	microfibril-associated glycoproteins
Micro-CT	micro-computed tomography
MTT	3-(4,5-dimethyl-2-thiazolyl)-2,5-diphenyl-2H-tetrazolium bromide
Maleimide-PEG- NHS	α-maleimide-ω-N-hydroxysuccinimide ester poly (ethylene glycol)
NPs	nanoparticles
PBS	phosphate buffered saline
PLA	polylactic acid
PLGA	poly (lactic-co-glycolic) acid
RASMCs	rat aortic smooth muscle cells
SEM	standard error of the mean
TACT	Trial to Assess Chelation Therapy
TEM	transmission electron microscope
UV–vis	ultraviolet–visible
VCAM-1	vascular cell adhesion molecule-1
VSMCs	vascular smooth muscle cells

Supplementary data to this article can be found online at http://dx.doi.org/10.1016/j.jconrel.2014.09.029.

Funding

This work was supported by NIH P20GM103444 grant and the Hunter Endowment at Clemson University to Dr. Naren Vyavahare.

Acknowledgments

The authors would like to thank Dr. Haijun Qian at Clemson University Electron Microscopy Laboratory (Anderson, SC) for TEM work; Dr. Michael E. Ward at Greenville Health System (Greenville, SC) for providing samples of calcified human aorta; Dr. Terri Bruce and Ms. Rhonda Powell at Clemson Light Imaging Facility of Clemson University for Leica M80 stereo microscope work; Dr. Jonathon Nye, Ms. Margie Jones, and Dr. Baowei Fei at Center for Systems Imaging, Emory University School of Medicine, for Micro-CT work; Dr. David Kwartowitz, Mr. Michael Jaeggli, and Ms. Siyu Ma at Clemson University for Micro-CT data analysis using Mevislab software; Mr. Luke Pietrykowski at the Clemson University Biomedical Engineering Innovation Campus (Greenville, SC) for mechanical testing using Bose Electroforce 3200; Dr.John Parrish, Mr. Travis Pruitt, Ms. Tina Parker, and Ms. Stefanie Pardue at Clemson University's Godley-Snell Research Center for animal work; Mr. Saketh Karamched, Mr. Vaideesh Parasaram, Mr. Hobey Tam, and Ms. Linae Maganini for animal surgery and organ harvest; and Mr. Andrew Holman for manuscript edits.

References

[1] D. Proudfoot, C.M. Shanahan, Biology of calcification in vascular cells: intima versus media, Herz 26 (2001) 245–251.
[2] K. Boström, L.L. Demer, Regulatory mechanisms in vascular calcification, Crit. Rev. Eukaryot. Gene Expr. 10 (1999) 151–158.
[3] A.I. MacIsaac, T.A. Bass, M. Buchbinder, M.J. Cowley, M.B. Leon, D.C. Warth, P.L. Whitlow, High speed rotational atherectomy: outcome in calcified and noncalcified coronary artery lesions, J. Am. Coll. Cardiol. 26 (1995) 731–736.
[4] J.S. Coselli, L.D. Conklin, S.A. LeMaire, Thoracoabdominal aortic aneurysm repair: review and update of current strategies, Ann. Thorac. Surg. 74 (2002) S1881–S1884.
[5] T.D. Fraker, S.D. Fihn, 2007 Chronic Angina Focused Update of the ACC/AHA 2002 Guidelines for the Management of Patients With Chronic Stable AnginaA Report of the American College of Cardiology/American Heart Association Task Force on Practice Guidelines Writing Group to Develop the Focused Update of the 2002 Guidelines for the Management of Patients With Chronic Stable Angina, J. Am. Coll. Cardiol. 50 (2007) 2264–2274.
[6] K.C. Atwood IV, E. Woeckner, R.S. Baratz, W.I. Sampson, Why the NIH Trial to Assess Chelation Therapy (TACT) should be abandoned, Medscape J. Med. 10 (2008) 115.
[7] G.A. Lamas, C. Goertz, R. Boineau, D.B. Mark, T. Rozema, R.L. Nahin, J.A. Drisko, K.L. Lee, Design of the Trial to Assess Chelation Therapy (TACT), Am. Heart J. 163 (2012) 7–12.
[8] G.A. Lamas, C. Goertz, R. Boineau, et al., Effect of disodium edta chelation regimen on cardiovascular events in patients with previous myocardial infarction: The tact randomized trial, JAMA 309 (2013) 1241–1250.
[9] B. Guldager, K. Brixen, S. Jørgensen, H. Nielsen, L. Mosekilde, R. Jelnes, Effects of intravenous EDTA treatment on serum parathyroid hormone (1–84) and biochemical markers of bone turnover, Dan. Med. Bull. 40 (1993) 627–630.
[10] J.F. Holland, E. Danielson, A. Sahagian-Edwards, Use of ethylene diamine tetra acetic acid in hypercalcemic patients, Exp. Biol. Med. 84 (1953) 359–364.
[11] A. Pasch, T. Schaffner, U. Huynh-Do, B.M. Frey, F.J. Frey, S. Farese, Sodium thiosulfate prevents vascular calcifications in uremic rats, Kidney Int. 74 (2008) 1444–1453.
[12] Y. Lei, A. Grover, A. Sinha, N. Vyavahare, Efficacy of reversal of aortic calcification by chelating agents, Calcif. Tissue Int. 93 (2013) 426–435.
[13] Y. Lei, Mechanisms and reversal of elastin specific arterial calcification, Department of Bioengineering, Clemson University, Clemson, SC, 2014. 111–127 (PhD Dissertation).
[14] R. Singh, J.W. Lillard Jr., Nanoparticle-based targeted drug delivery, Exp. Mol. Pathol. 86 (2009) 215–223.
[15] A. Sinha, A. Shaporev, N. Nosoudi, Y. Lei, A. Vertegel, S. Lessner, N. Vyavahare, Nanoparticle targeting to diseased vasculature for imaging and therapy, Nanomedicine: NBM 5 (2014) 1003–10012.
[16] K. Langer, S. Balthasar, V. Vogel, N. Dinauer, H. Von Briesen, D. Schubert, Optimization of the preparation process for human serum albumin (HSA) nanoparticles, Int. J. Pharm. 257 (2003) 169–180.
[17] A.O. Elzoghby, W.M. Samy, N.A. Elgindy, Albumin-based nanoparticles as potential controlled release drug delivery systems, J. Control. Release 157 (2012) 168–182.
[18] H. Wartlick, K. Michaelis, S. Balthasar, K. Strebhardt, J. Kreuter, K. Langer, Highly specific HER2-mediated cellular uptake of antibody-modified nanoparticles in tumour cells, J. Drug Target. 12 (2004) 461–471.
[19] J.S. Lee, D.M. Basalyga, A. Simionescu, J.C. Isenburg, D.T. Simionescu, N.R. Vyavahare, Elastin calcification in the rat subdermal model is accompanied by up-regulation of degradative and osteogenic cellular responses, Am. J. Pathol. 168 (2006) 490–498.
[20] D.M. Basalyga, D.T. Simionescu, W. Xiong, B.T. Baxter, B.C. Starcher, N.R. Vyavahare, Elastin degradation and calcification in an abdominal aorta injury model role of matrix metalloproteinases, Circulation 110 (2004) 3480–3487.
[21] P.A. Price, S.A. Faus, M.K. Williamson, Warfarin causes rapid calcification of the elastic lamellae in rat arteries and heart valves, Arterioscler. Thromb. Vasc. Biol. 18 (1998) 1400–1407.
[22] J. Hanken, R. Wassersug, A new double-stain technique reveals the nature of the hard tissues, Funct. Photog 16 (1981) 22–26.
[23] E. Rosa-Molinar, B. Proskocil, M. Ettel, B. Fritzsch, Whole-mount procedures for simultaneous visualization of nerves, neurons, cartilage and bone, Brain Res. Protocol. 4 (1999) 115–123.
[24] V. Persy, A. Postnov, E. Neven, G. Dams, M. De Broe, P. D'Haese, N. De Clerck, High-resolution X-ray microtomography is a sensitive method to detect vascular calcification in living rats with chronic renal failure, Arterioscler. Thromb. Vasc. Biol. 26 (2006) 2110–2116.
[25] A.A. Postnov, P.C. D'Haese, E. Neven, N.M. Clerck, V.P. Persy, Possibilities and limits of X-ray microtomography for in vivo and ex vivo detection of vascular calcifications, Int. J. Cardiovasc. Imaging 25 (2009) 615–624.
[26] N. Vyavahare, M. Ogle, F.J. Schoen, R.J. Levy, Elastin calcification and its prevention with aluminum chloride pretreatment, Am. J. Pathol. 155 (1999) 973–982.
[27] S.L. Schwartz, J.R. Hayes, R.S. Ide, C.B. Johnson, P.D. Doolan, Studies of the nephrotoxicity of ethylenediaminetetraacetic acid, Biochem. Pharmacol. 15 (1966) 377–389.
[28] P.D. Doolan, S.L. Schwartz, J.R. Hayes, J.C. Mullen, N.B. Cummings, An evaluation of the nephrotoxicity of ethylenediaminetetraacetate and diethylenetriaminepentaacetate in the rat, Toxicol. Appl. Pharmacol. 10 (1967) 481–500.
[29] S.L. Schwartz, C.B. Johnson, P.D. Doolan, Study of the mechanism of renal vacuologenesis induced in the rat by ethylenediaminetetraacetate comparison of the cellular activities of calcium and chromium chelates, Mol. Pharmacol. 6 (1970) 54–60.
[30] E. McDonagh, C. Rudolph, E. Cheraskin, The effect of EDTA chelation therapy plus supportive multivitamin-trace mineral supplementation upon renal function: a study in serum creatinine, J. Holist. Med. 4 (1982) 146–151.
[31] L. Oliver, R. Mehta, H. Sarles, Acute renal failure following administration of ethylenediamine-tetraacetic acid (EDTA), Tex. Med. 80 (1984) 40.
[32] M.J. Hawkins, P. Soon-Shiong, N. Desai, Protein nanoparticles as drug carriers in clinical medicine, Adv. Drug Deliv. Rev. 60 (2008) 876–885.
[33] B. Sivaraman, A. Ramamurthi, Multifunctional nanoparticles for doxycycline delivery towards localized elastic matrix stabilization and regenerative repair, Acta Biomater. 9 (2013) 6511–6525.
[34] E.C. Cho, L. Au, Q. Zhang, Y. Xia, The effects of size, shape, and surface functional group of gold nanostructures on their adsorption and internalization by cells, Small 6 (2010) 517–522.
[35] M. Nahrendorf, H. Zhang, S. Hembrador, P. Panizzi, D.E. Sosnovik, E. Aikawa, P. Libby, F.K. Swirski, R. Weissleder, Nanoparticle PET-CT imaging of macrophages in inflammatory atherosclerosis, Circulation 117 (2008) 379–387.
[36] D. Schrama, R.A. Reisfeld, J.C. Becker, Antibody targeted drugs as cancer therapeutics, Nat. Rev. Drug Discov. 5 (2006) 147–159.
[37] M.S. Kaminski, K.R. Zasadny, I.R. Francis, A.W. Milik, C.W. Ross, S.D. Moon, S.M. Crawford, J.M. Burgess, N.A. Petry, G.M. Butchko, Radioimmunotherapy of B-cell lymphoma with [131I] anti-B1 (anti-CD20) antibody, N. Engl. J. Med. 329 (1993) 459–465.
[38] P.A. Price, H.H. June, J.R. Buckley, M.K. Williamson, Osteoprotegerin inhibits artery calcification induced by warfarin and by vitamin D, Arterioscler. Thromb. Vasc. Biol. 21 (2001) 1610–1616.